Chapter 5

Testing the synchronous filter on experimental data

5.1 Introduction

In this chapter the synchronous filter for time domain averaging of gear vibration data that was developed in Chapter 4 is implemented on a new data set from the accelerated gear life test rig. The data set was measured at two-hour intervals throughout the gear life. Taking measurements over the entire gear life serves the purpose of demonstrating the suitability of the developed filter in predicting the time domain average over the entire gear life. Secondly, we want to evaluate the suitability of the developed synchronous filter for time domain averaging for use in cases where the applied load is not constant as would be the case in a typical industrial application. In this a brief background on the data is presented. This is followed by simulation using the developed models for MLP, RBF and SVM, respectively. The results are compared to those that are obtained using direct time domain averaging approach, focusing on the practical implications. The synchronous filter is also tested on data from a test conducted under varying load conditions.

5.2 Data representation

The gear was expected to have a life of 30 hours; therefore vibration measurements were taken in two-hour intervals until failure occurred so as to properly monitor the progression of gear failure. The data was sampled at a frequency of 51,2 kHz to get a full representation of the frequencies of interest, in our case, the gear mesh frequency (*GMF*) and its side bands (*SB*). The *GMF* is defined by

$$GMF = S_f \times N_T, \tag{5.1}$$

where S_f is the shaft frequency and N_T is the number of gear teeth. The side bands (*SB*) occur at a frequency F_r defined by

$$F_r = GMF - kS_f, \tag{5.2}$$

where k is an integer and S_f is the shaft frequency. For the accelerated gear life test rig the *GMF, SB* and operating properties are given in Table 5.1.

Table 5.1 Operating properties for test data (Davel, 2003)

Rotational Speed [revs/min]	***GMF* [Hz]**	***SB.1* [Hz]**	***SB.2* [Hz]**
311	223.0	217.2	228.2

From Table 5.1 it is observed that the highest frequency of interest is 228.2 Hz therefore the measured acceleration was low-pass filtered at 300 Hz. In a gearbox where the applied load is constant, the amplitude of the side bands of the meshing frequency (*SB*) and gear mesh frequency (*GMF*) in the frequency spectrum are expected to increase as the vibration increases. This observation supplies a means of representing the progression of gear life using gear vibration. In this work the *SB* is normalised with the *GMF* and then plotted over the gear life. Figure 5.1 shows the FFT spectrum of the measured vibration signals from one of the test signals. This plot clearly shows the *GMF* and *SB*.

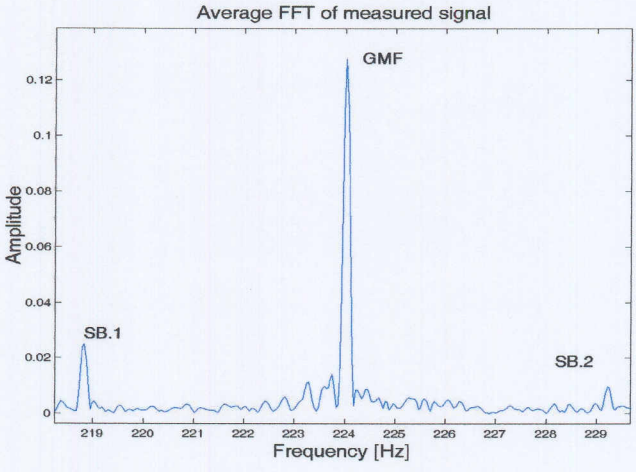

Figure 5.1 FFT plot measured acceleration signal after 9 hours in operation.

Figure 5.2 below shows the representation of the gear vibration over the entire gear life using normalised *SB.2*. This plot shows the normalised SB and a fourth order

polynomial fitted onto the normalised *SB* data. The fitted curve closely resembles the well known bath- tub curve (Norton, 1989) that models the life of most mechanical systems. The first 5 hours in operation show the running in stage of the gear life. The gear vibration level stabilises from 5 hours until 25 hours, which can be considered as constant gear wear stage. From 25 hours the gear vibration increases until the gear fails after 33 hours. The final stage can be considered as the wear out stage of the gear life.

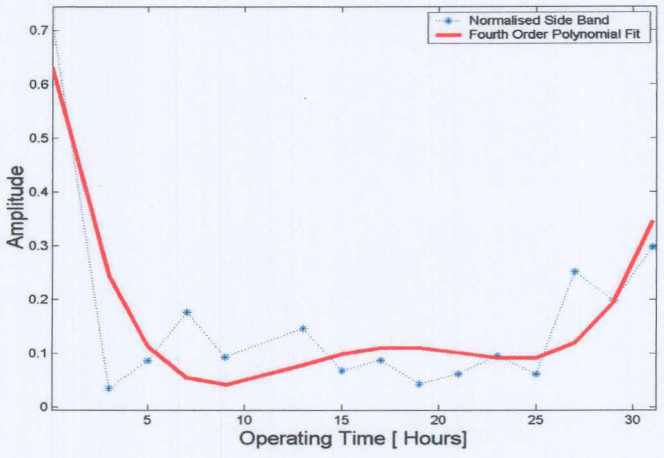

Figure 5.2 Testing data representation

In this chapter data sets from different stages of the gear life are used.

5.3 Model 1

This paragraph presents the results obtained using Model 1 for test data obtained from different stages of the gear life for tests conducted under constant load conditions as presented by Table 4.2. Model 1 with MLP, RBF and SVM formulations is tested and the results obtained for each of the formulations are compared to the TDA calculated using the direct time domain averaging approach after 160 gear rotations. For Model 1, 40 gear rotations are considered as the optimum number of inputs as discussed in Chapter 4. This is a reduction of 75 percent of the data that would be used when the direct averaging approach is used to calculate the TDA.

5.3.1 Model 1 with MLP feedforward network

Figure 5.3 (a) to Figure 5.3 (c) shows the prediction from Model 1 with MLP feedforward networks superimposed on the time domain average (TDA) of the gear vibration signals obtained using direct averaging. The simulations were done using

unseen validation sets as presented in Table 4.3. From Figure 5.3 (a) to Figure 5.3 (c), it is observed that Model 1 with MLP feedforward networks can correctly predict with 40 gear rotations the TDA for 160 gear rotations over the entire gear life. The FFT of the TDA calculated by direct averaging and the FFT of the simulation results are exact fits throughout the life of the gear. This indicates that Model 1 with MLP feedforward networks retains the diagnostic enhancing capabilities of TDA.

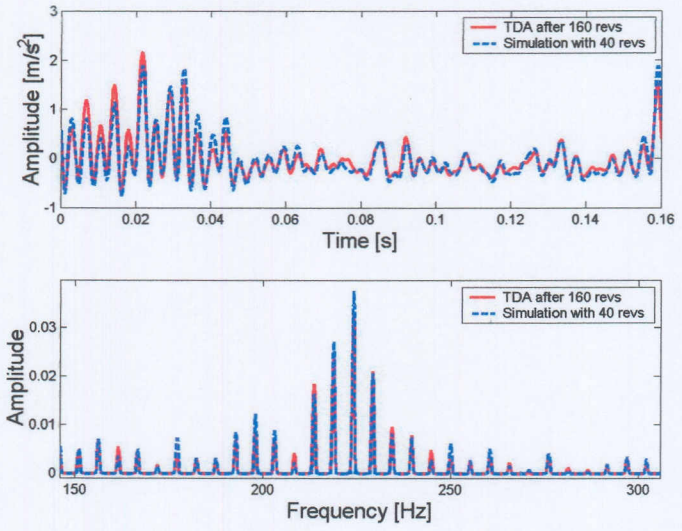

Figure 5.3 (a) Model 1 prediction with validation set of 40 gear rotations superimposed on the TDA from 160 rotations. The measurements were taken during the running in stage of the gear.

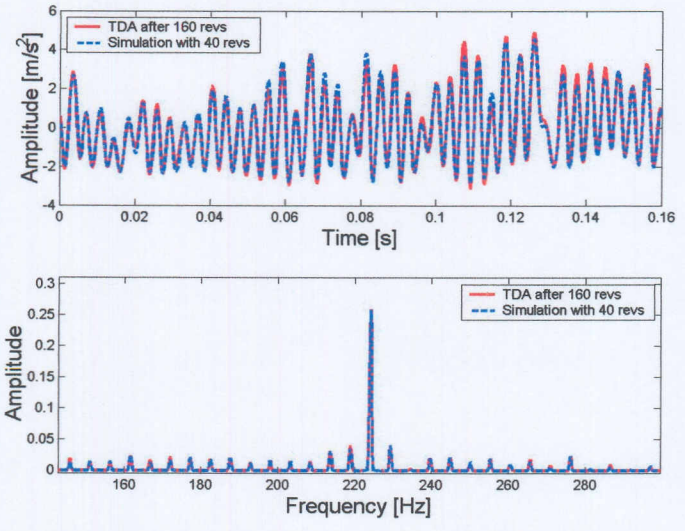

Figure 5.3 (b) Model 1 prediction with validation set of 40 gear rotations superimposed on the TDA from 160 rotations. The measurements were taken during the constant wear in stage of the gear.

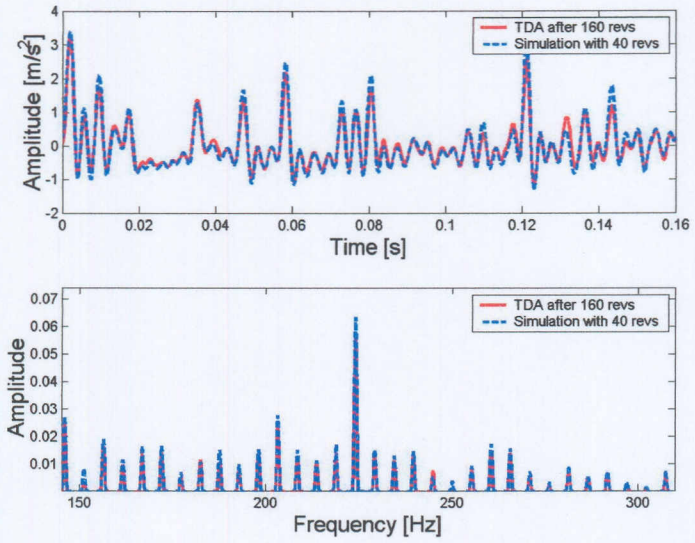

Figure 5.3 (c) Model 1 prediction with validation set of 40 gear rotations superimposed on the TDA from 160 rotations. The measurements were taken in the wear out stage of the gear.

5.3.2 Model 1 with RBF Feedforward network

Figure 5.4 (a) to Figure 5.4 (c) show the prediction of Model 1 with RBF feedforward neural networks. The simulation results are superimposed on the TDA of the gear vibration signals calculated using the direct averaging. The validation set had 40 inputs.

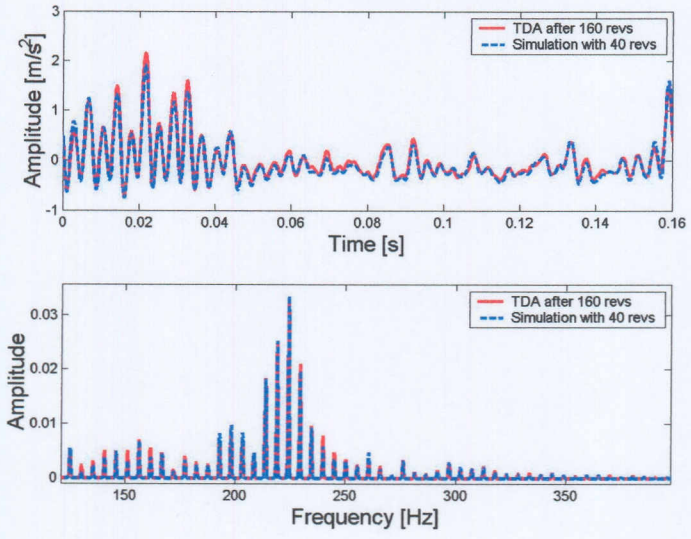

Figure 5.4 (a) Model 1 prediction with validation set of 40 gear rotations superimposed on the TDA from 160 rotations. The measurements were taken during the running in stage of the gear.

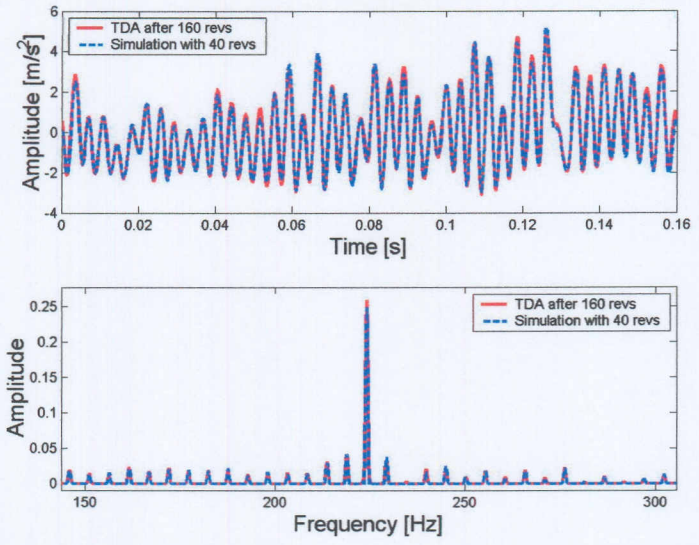

Figure 5.4 (b) Model 1 prediction with validation set of 40 gear rotations superimposed on the TDA after 160 rotations. The measurements were taken during the constant wear stage of the gear.

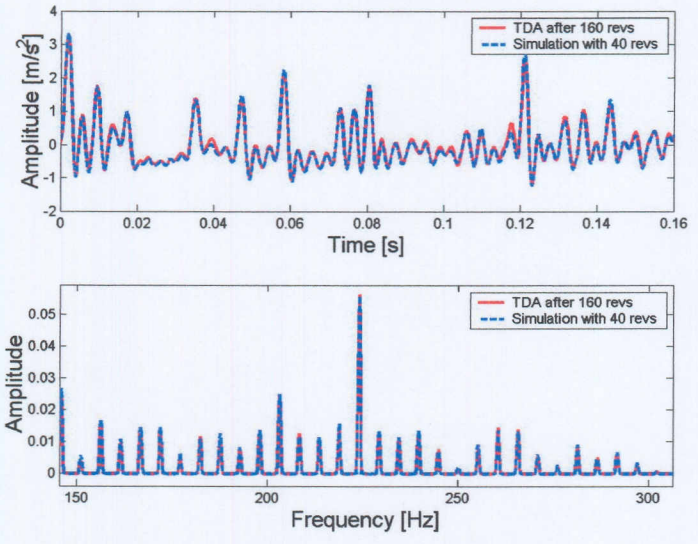

Figure 5.4 (c) Model 1 prediction with validation set of 40 gear rotations superimposed on the TDA after 160 rotations. The measurements were taken during the wear out stage of the gear.

The above plots show in both frequency domain and time domain representation, that Model 1 with a RBF feedforward network with 40 gear rotations can correctly predict the TDA for 160 gear rotations over the entire life of the gear. This is because the selected RBF network can effectively map the input to the output space. The FFT of the TDA calculated by direct averaging and the FFT of the simulation results are exact fits

throughout the life of the gear. This indicates that Model 1 with RBF feedforward networks retains the diagnostic enhancing capabilities of TDA.

5.3.3 Model 1 with SVMs

Figure 5.5 (a) to Figure 5.5 (c) show the prediction obtained using Model 1 with SVMs superimposed on the TDA of the gear vibration signals calculated by direct averaging. The following plots show the Model 1 with SVMs with an input of 40 gear rotation signals can correctly predict the TDA for 160 gear rotations over the entire life of the gear.

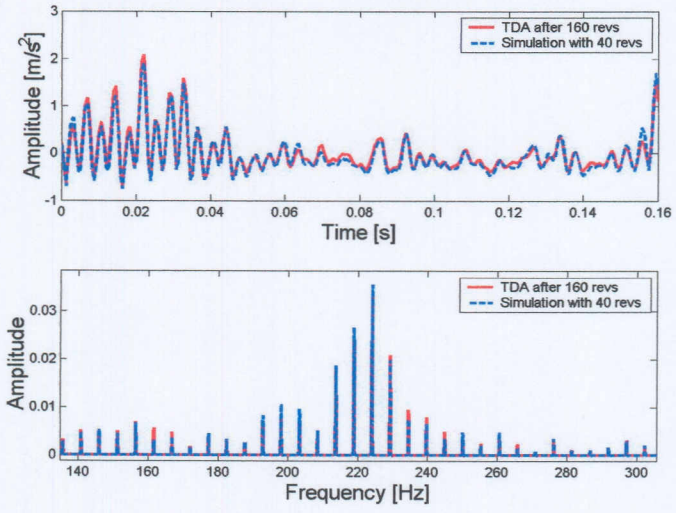

Figure 5.5 (a) Model 1 prediction with validation set of 40 gear rotations superimposed on the TDA for 160 rotations. The measurements were taken during the running in stage of the gear.

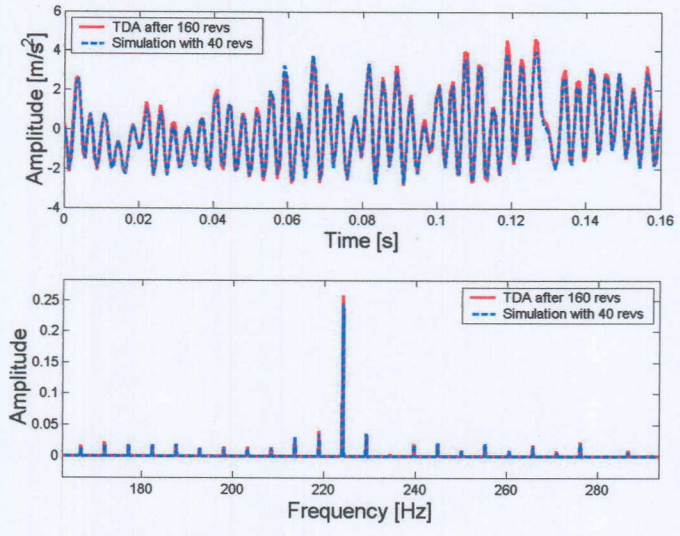

Figure 5.5 (b) Model 1 prediction with validation set of 40 gear rotations superimposed on the TDA obtained after 160 rotations. The measurements were from the constant wear gear stage.

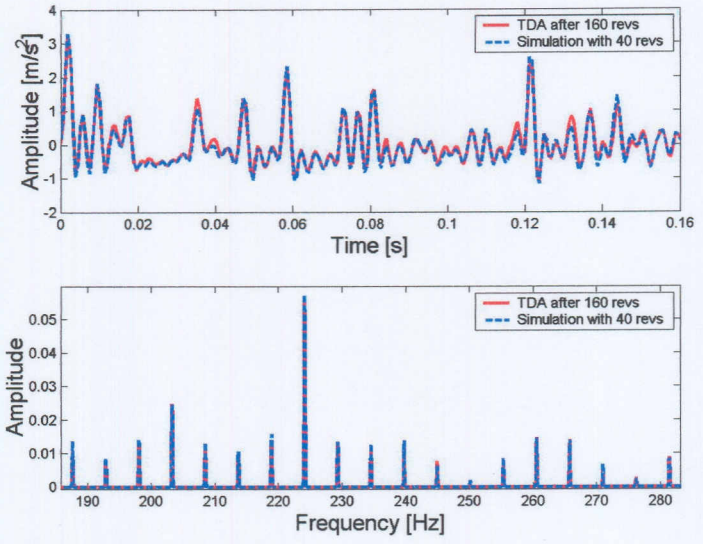

Figure 5.5 (c) Model 1 prediction with validation set of 40 gear rotations superimposed on the TDA after 160 rotations. The measurements were taken from the wear out stage of the gear.

The FFT of the TDA calculated by direct averaging and the FFT of the simulation results are exact fits throughout the life of the gear. This indicates that Model 1 with SVMs retains the diagnostic enhancing capabilities of TDA. The good performance of SVMs is due to their superior ability to train and generalise (Gunn, 1998).

5.4 Model 2

This paragraph presents the results obtained using Model 2 from measurements taken at different stages of the gear life. The measurements were taken while the gearbox was operating under constant load conditions. Model 2 with MLP, RBF and SVMs is simulated with unseen validation data sets as presented in Table 4.4. The obtained results for each of the formulations are compared to the TDA calculated using the direct averaging for 160 gear rotations. In Model 2 all 160 rotation synchronised gear vibration signals are sequentially used in batches of 10 rotations. The rotation signals that have already been passed through the first stage of the model are deleted from the memory of the data acquisition system, while their output is saved for use in the second stage of the model. After simulation with all 160 gear rotations, there are 16 signals that will be stored in the data acquisition system. This means that the highest number of signals that will be stored in the data acquisition system is 1 batch of 10 signals and 16 outputs from the first stage of Model 2. This results in 26 signals instead of 160 rotation

synchronised gear vibration signals. This is effectively a reduction of 83.75 % of the data that needs to be stored in the data acquisition system during the time domain averaging process for this test data set.

5.4.1 Model 2 with MLP feedforward network

Figure 5.6 (a) to Figure 5.6 (c) show the prediction from Model 2 with MLP feedforward networks superimposed on TDA of the gear vibration signals calculated using direct averaging.

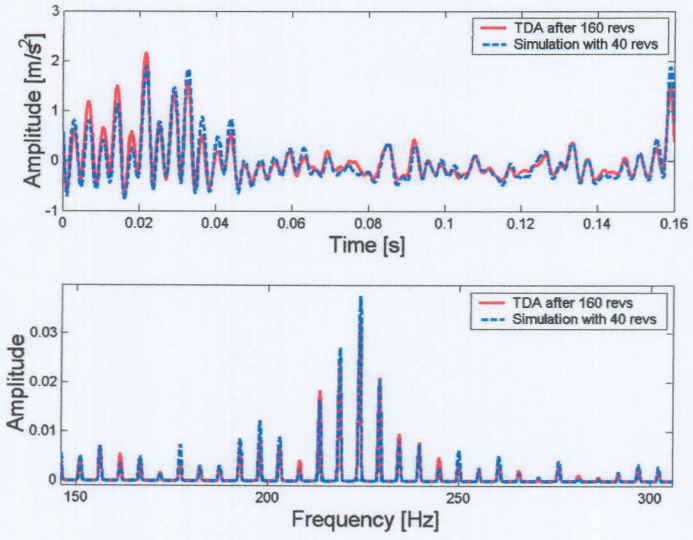

Figure 5.6 (a) Model 2 prediction with a validation set measured during the running in stage of the gear life superimposed on the TDA calculated with 160 gear rotations.

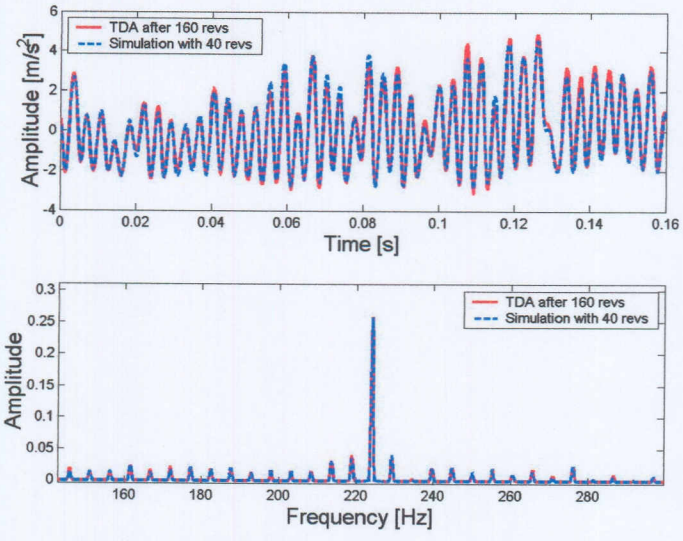

Figure 5.6 (b) Model 2 prediction with a validation set measured during the constant wear stage of the gear life superimposed on the TDA calculated with 160 gear rotations.

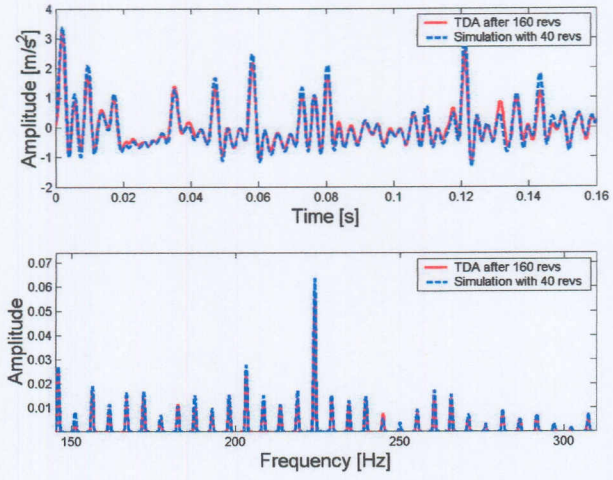

Figure 5.6 (c) Model 2 prediction with a validation set measured during the wear out stage of the gear life superimposed on the TDA calculated with 160 gear rotations.

The above plots show in both frequency domain and time domain representation, that Model 2 with a MLP feedforward network can correctly predict the TDA for 160 gear rotations over the entire life of the gear. This is because in model 2 the network is exposed to the entire data set, therefore, it simulates more effectively.

5.4.2 Model 2 with RBF feedforward network

Figure 5.7 (a) to Figure 5.7 (c) show the prediction from Model 2 with RBF feedforward networks superimposed on the TDA of the gear vibration signals calculated using direct averaging.

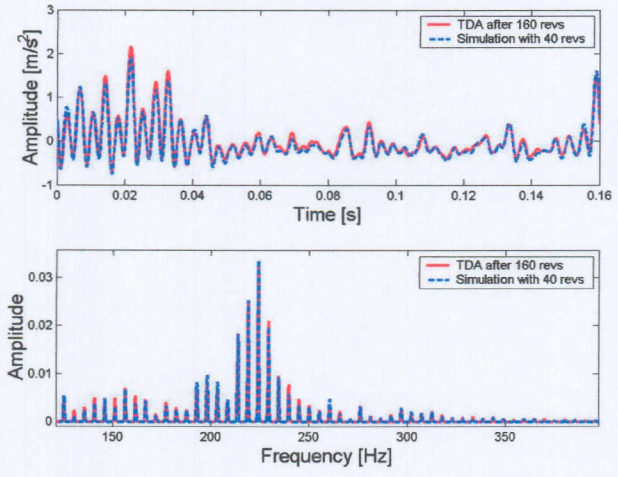

Figure 5.7 (a) Model 2 prediction with a validation set measured during the running in stage of the gear life superimposed on the TDA calculated with 160 gear rotations.

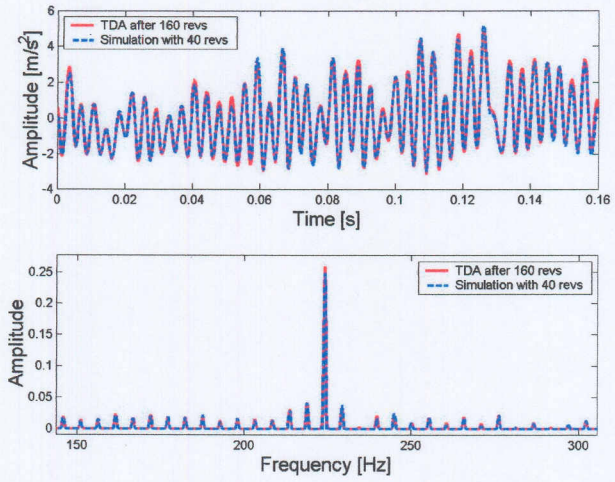

Figure 5.7 (b) Model 2 prediction with a validation set measured during the constant wear stage of the gear life superimposed on the TDA calculated with 160 gear rotations.

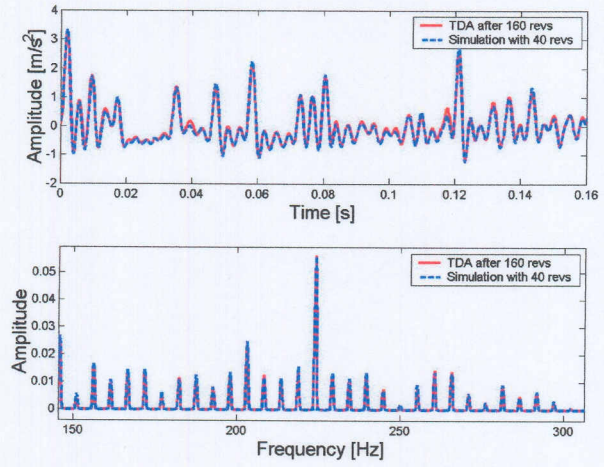

Figure 5.7 (c) Model 2 prediction with a validation set measured during the wear out stage of the gear life superimposed on the TDA calculated with 160 gear rotations.

Figure 5.7 (a) to Figure 5.7 (c) show that Model 2 with a RBF feedforward network can correctly predict the TDA for 160 gear rotations over the entire gear life. This is because in Model 2 the network is exposed to the entire data set, therefore, it simulates more effectively.

5.4.3 Model 2 with SVMs

Figure 5.8 (a) to Figure 5.8 (c) show the prediction from Model 2 with SVMs superimposed on the TDA of the gear vibration signals calculated using the direct averaging.

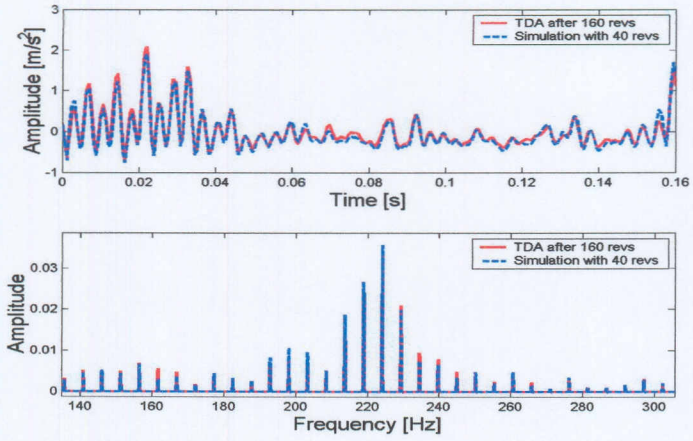

Figure 5.8 (a) Model 2 prediction with a validation set measured during the running in stage of the gear life superimposed on the TDA calculated with 160 gear rotations.

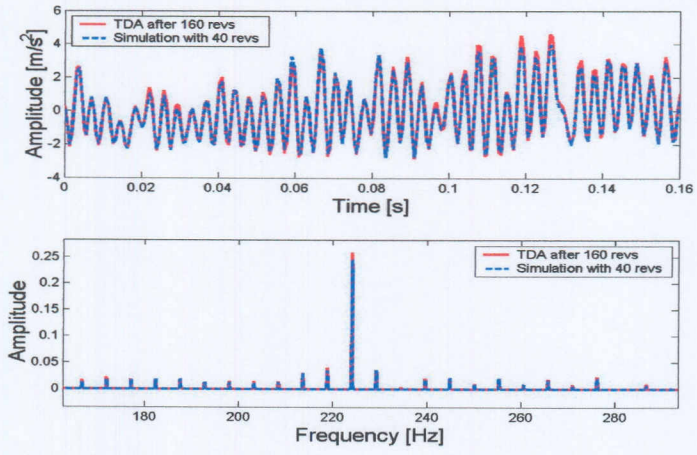

Figure 5.8 (b) Model 2 prediction with a validation set measured during the constant wear stage of the gear life superimposed on the TDA calculated with 160 gear rotations.

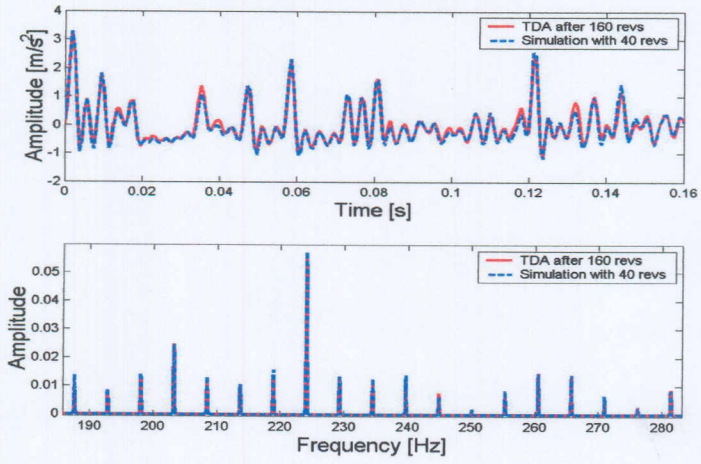

Figure 5.8 (c) Model 2 prediction with a validation set measured during the wear out stage of the gear life superimposed on the TDA calculated with 160 gear rotations.

Figure 5.8 (a) to Figure 5.8 (c) show that Model 2 with a SVM feedforward network can correctly predict the TDA for 160 gear rotations over the entire life of the gear.

5.4.4 Discussion

In Figures 5.3 (a) to Figure 5.8 (a) it is observed that the TDA of the vibration from the running in stage of the gear life is fairly random. The amplitude of the TDA in the running in stage of the gear life is less than the amplitude of the TDA in the other two stages of the gear life. The random noise content of the vibration results in the presence of prominent side bands as observed frequency spectrums in Figures 5.3 (a) to Figure 5.8 (a). In Figures 5.3 (b) to Figure 5.8 (b) it is observed that the amplitude of the TDA increased and the signal is more periodic because of the constant loading condition. The reduced random noise in the signal is shown by the reduction in the side bands of the gear mesh frequency observed in the frequency spectrums in Figures 5.3 (b) to Figure 5.8 (b). Figures 5.3 (c) to Figure 5.8 (c) show an increase in the amplitude of the TDA. This is expected as one would expect the vibration would to increase as the gear fails. There is also evidence of impulse in the TDA signal. This may be because some of the gear teeth may have cracked resulting in the reduction of the meshing stiffness of those meshing tooth sets. The introduction of impulses in the TDA results in the increase in the side bands of the gear mesh frequency as observed in Figures 5.3 (c) to Figure 5.8 (c).

5.5 Assessing simulation accuracy and diagnostic capabilities

Up to this point the developed models have been used to predict the TDA of the gear vibration signal without quantifying the quality of the prediction and the diagnostic capability of the model outputs. This section presents some parameters that will be used to assess the quality of the prediction and establish whether the model predictions retain the diagnostic capabilities of the TDA.

To quantify the quality the simulation accuracy a 'fit' parameter η_{sim} (Raath, 1992) is defined. First the response error is defined as

$$e_{sim}(k) = y_{desired}(k) - y_{achieved}(k), \tag{5.3}$$

Assume that we have N data points. The simulation accuracy may then be defined as

$$\eta_{sim} = 100 \frac{\sum_{k=1}^{N} |e(k)|}{\sum_{k=1}^{N} |y_{desired}(k)|} \quad [\%] \tag{5.4}$$

The defined 'fit' parameter η_{sim} is attractive in that it gives a single value for each simulation, therefore it can be used to compare the performance of the different formulations over the entire life of the gear. A low value of 'fit' parameter η_{sim} implies a good fit while a high value implies a bad fit, therefore, a 'fit' parameter value of $\eta_{sim} = 0\%$ implies a perfect fit. In this work it was established experimentally that $\eta_{sim} = 40\%$ is a suitable upper cut-off of the simulation accuracy.

To establish whether the model predictions retain the diagnostic capabilities of the TDA two parameters are used. The first parameter is the peak value of the vibration X_{max} during a given interval T. This parameter can be used where the analyst is interested only in the overall magnitude of the vibration to distinguish between acceptable and unsatisfactory vibration states (Heyns, 2002). The second parameter is the kurtosis. The kurtosis is the fourth statistical moment of the vibration signal and it is given by

$$\text{kurtosis} = \frac{1}{\sigma^4 T} \int_0^T x^4 dt. \tag{5.5}$$

where T is a given interval, σ is the variance and x is the vibration data. The kurtosis of a signal is very useful for detecting the presence of an impulse within the signal (Norton, 1989). The peak value of the vibration X_{max} and the kurtosis of the TDA calculated using direct averaging is compared to the TDA from Model 1 and Mode 2 with all three formulations.

5.5.1 Comparison of the performance of the different formulations

The performance of the three formulations in Model 1 and Model 2 was assessed using the fit parameter to determine which of the formulations is best suited for this

application. Figure 5.9 shows the simulation accuracy η_{sim} plotted against the gear life for Model 1.

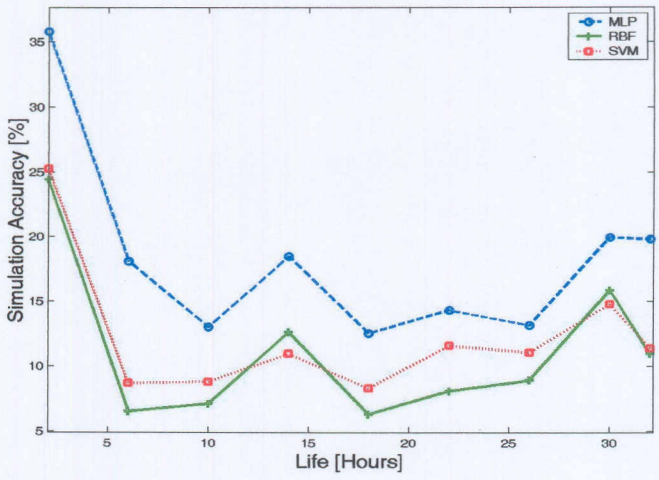

Figure 5.9 Model 1 Simulation Accuracy η_{sim} vs. gear life.

From this plot it is observed that the performance Model 1 with RBF network and Model 1 with SVMs is the same. Their performance is slightly better than the performance of Model 1 with MLP networks. The performances of all three formulations are acceptable because η_{sim} is less than the cut-off value for all the formulations.

Figure 5.10 shows the simulation accuracy η_{sim} plotted against the gear life for Model 2.

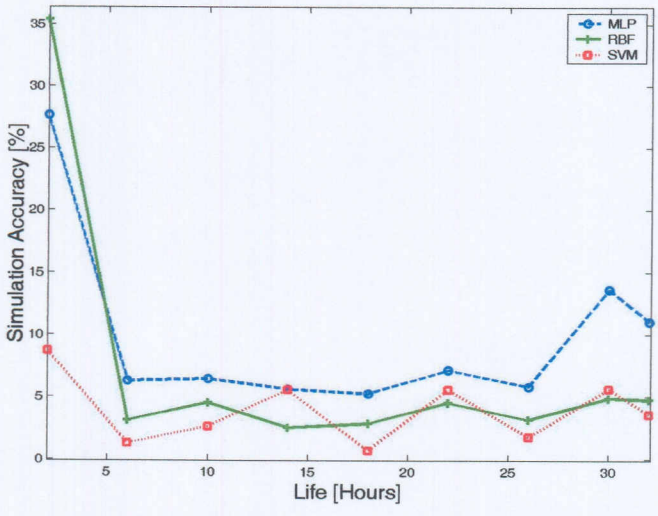

Figure 5.10 Model 2 Simulation Accuracy η_{sim} vs. gear life.

From Figure 5.10 it is observed that the performance of the formulations for Model 2 is practically the same. The performances of all three formulations are acceptable because η_{sim} is less than the cut-off value for all the formulations.

Next the performance of Model 1 and Mode 2 for each of the formulation is assessed. Figure 5.11 shows the performance of the two models with MLP feedforward networks.

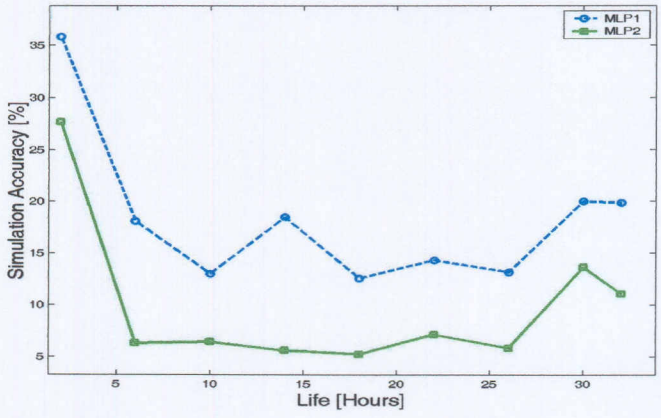

Figure 5.11 Performance of Model 1 and Model 2 with MLP feedforward networks.

From Figure 5.11 it is observed that Model 2 performs better than Model 1. This is because when simulating with Model 2 the whole data set is used as opposed to Model 1 in which only a section of the data is used.

Figure 5.12 shows the performance of the two models with RBF feedforward networks.

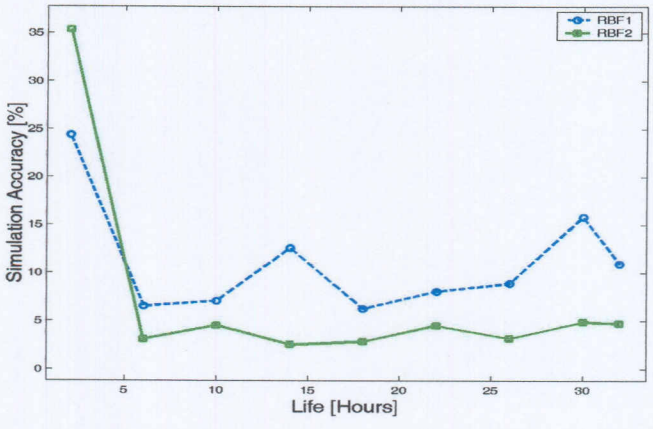

Figure 5.12 Performance of Model 1 and Model 2 with RBF feedforward networks.

Figure 5.12 shows that for RBF networks Model 1 performs better than that Model 2 in the running in stages of the gear life. After this stage the performance of Model 2 is

better than the performance of Model 1. This is because the vibration signature in the running in stages of the gear is much different to the vibration during the rest of the gear life as discussed in Section 5.4.4.

Figure 5.13 shows the performance of the two models with SVM. From this plot it is observed that Model 2 performs much better than Model 1. This is because although the vibration signatures in different stages of the gear life are different, the SVM has good generalisation properties and also the fact that when simulating with Model 2 the whole data set is used.

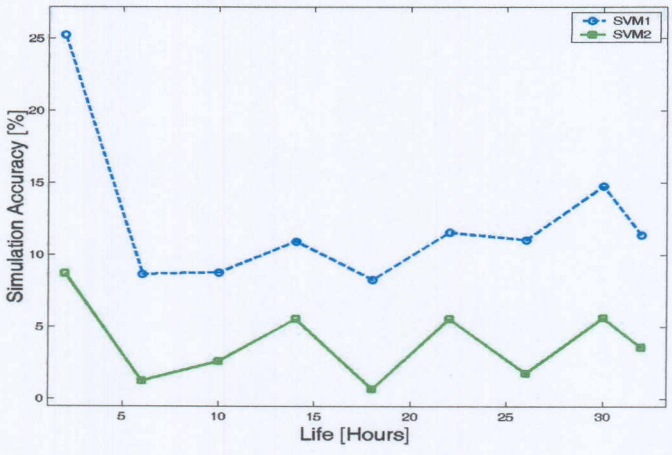

Figure 5.13 Performance of Model 1 and Model 2 with SVM.

From Figure 5.11 to Figure 5.13 it is concluded that the performances of Model 1 and Model 2 for the different formulations are quite comparable over the whole life of the gear tested under constant load conditions.

5.5.2 Comparison of the diagnostic properties of the TDA calculated by direct averaging and the TDA predicted by the developed models

To establish whether the TDA predicted by the developed models retain the diagnostic capabilities of the TDA calculated by direct averaging the peak value X_{max} and the kurtosis are used. Figure 5.14 and Figure 5.15 are plots of X_{max} and kurtosis calculated from the TDA predicted by the developed models superimposed on the X_{max} and kurtosis calculated from the TDA obtained using direct averaging for data measured under constant loading conditions. Figure 5.14 shows the results obtained using Model 1 for MLP, RBF and SVMs throughout the life of the gear.

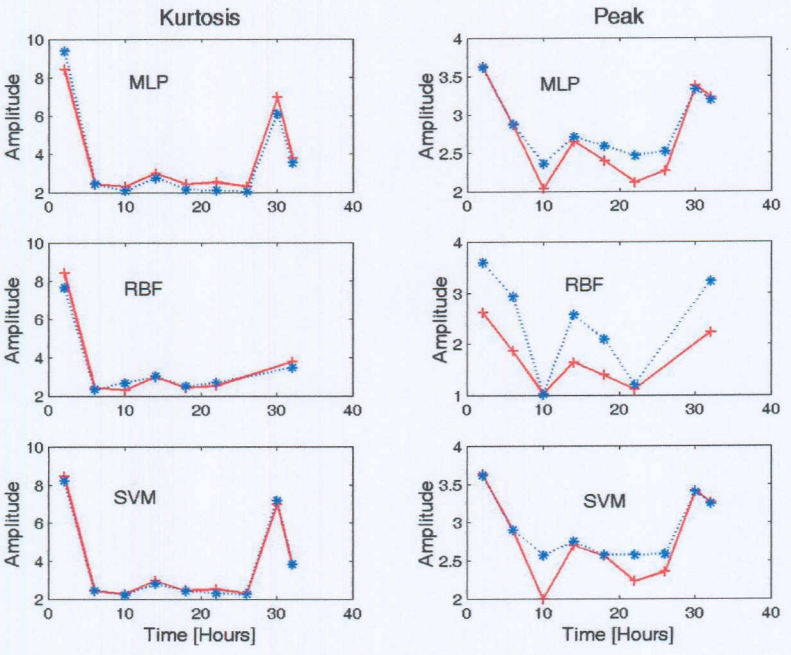

Figure 5.14 Comparison of kurtosis and peak values for the TDA calculated by direct averaging (solid line) and the TDA predicted by Model 1 (dotted line) with MLP, RBF and SVMs.

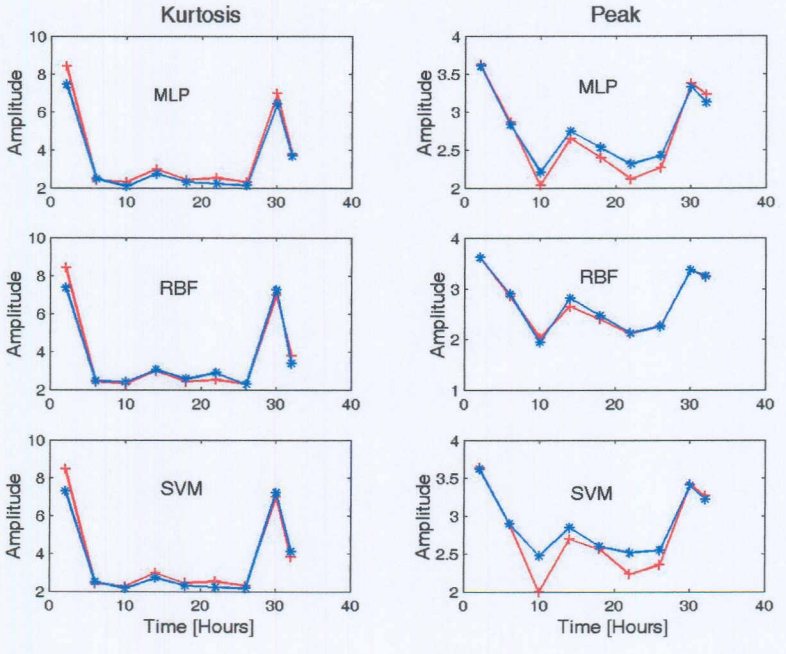

Figure 5.15 Comparison of kurtosis and peak values for the TDA calculated by direct averaging (solid line) and the TDA predicted by Model 2 (dotted line) with MLP, RBF and SVMs.

From Figure 5.14 it is observed that for all three formulations the kurtosis is an almost exact fit. This implies that the TDA predicted by Model 1 can be used to monitor the presence of impulses in the gear vibration. It is observed from this plot that there are

lots of impulses in the gear vibration during the running in and wear out stages of the gear life. On the other hand, only the peak values obtained from Model 1 with MLP and SVM are close fits and can be used to monitor the amplitude of the overall vibration. The bad performance of Model 1 with RBF is because the RBF network selected in this simulation was not optimal, therefore generalised badly to changes in the measured vibration as gear failure progressed.

Figure 5.15 shows the results obtained using Model 2 for MLP, RBF and SVMs throughout the life of the gear. It is observed from Figure 5.16 that for all three formulations the kurtosis is an exact fit therefore the TDA predicted by Model 1 can be used to monitor the presence of impulses in the gear vibration. The peak values obtained for all three formulations are close fits, therefore they can be used to monitor the amplitude of the overall vibration. The better performance on the peak values is because Model 2 uses the entire gear vibration during its simulation, therefore the network is exposed to all the underlying dynamics within the measured vibration.

5.6 Performance of developed models under varying load conditions

This topic of gearboxes operating under varying load conditions has been studied in great detail. Stander and Heyns (2001) noted the influence of varying loads on vibration monitoring of gears. Stander et al. (2002)[b] conducted an experimental investigation to observe the influence of fluctuating load conditions on the measured acceleration signal. They concluded that the load variation manifests itself as a low-frequency modulation on the measured acceleration signal. In this section the performance of the developed model for time domain averaging on data obtained from test conducted under varying load conditions is assessed. A random load with frequencies varying between 2 Hz and 5 Hz was applied. Measurements were taken at three different stages of the gear life, the running in stage, the constant wear stage and the wear out stage. The acquired data was processed as described in Chapter 4 and simulations were done using unseen validation sets for Model 1 and Model 2.

5.6.1 Simulations with Model 1

This paragraph presents the results obtained using Model 1 for test data obtained from different stages of the gear life of tests conducted under varying load conditions. Figure

5.16 (a) to Figure 5.16 (c) show the results obtained when Model 1 with MLP network is simulated with a validation set of 40 unseen gear rotations for the three different gear life stages.

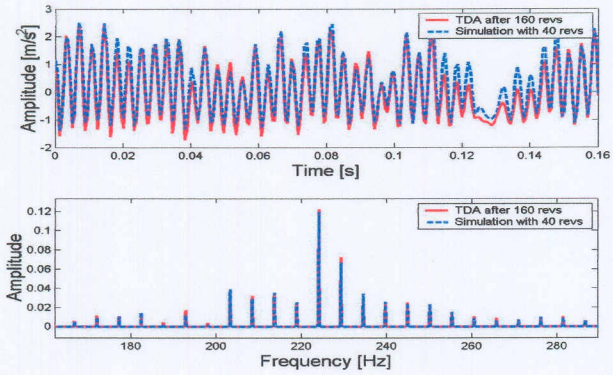

Figure 5.16 (a) Model 1 prediction with validation set of 40 gear rotations superimposed on the TDA from 160 rotations from measurements taken during the running in stage of the gear.

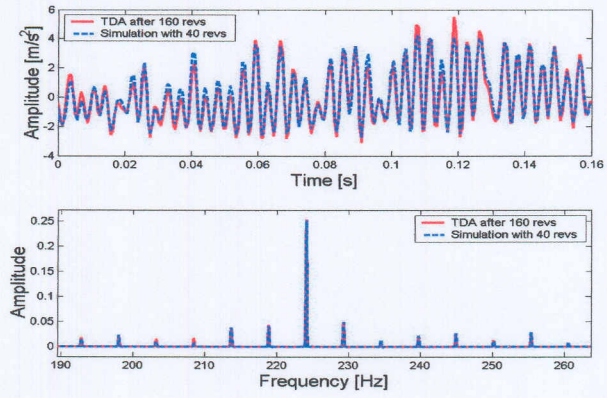

Figure 5.16 (b) Model 1 prediction with validation set of 40 gear rotations superimposed on the TDA from 160 rotations from measurements taken from the constant wear stage of the gear.

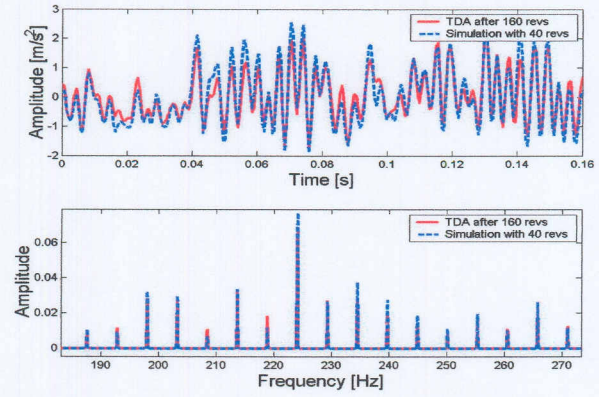

Figure 5.16 (c) Model 1 prediction with validation set of 40 gear rotations superimposed on the TDA from 160 rotations from measurements taken in the wear out stage of the gear.

The above plots show that Model 1 with 40 gear rotations can predict the TDA for 160 gear rotations fairly well over the different life stages of the gear under varying load conditions. This is because of the good generalisation capabilities of the MLP network. The frequency spectrum in this plot indicates that Model 1 with MLP can pick up the side bands of the gear mesh frequency.

Figure 17 (a) to Figure 17 (c) show the results obtained when Model 1 with RBF network is simulated using 40 unseen gear rotations for the three different gear life stages.

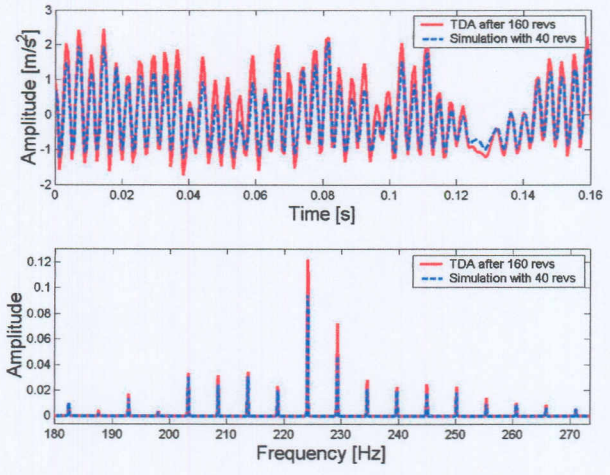

Figure 5.17 (a) Model 1 prediction with validation set of 40 gear rotations superimposed on the TDA from 160 rotations from measurements taken during the running in stage of the gear.

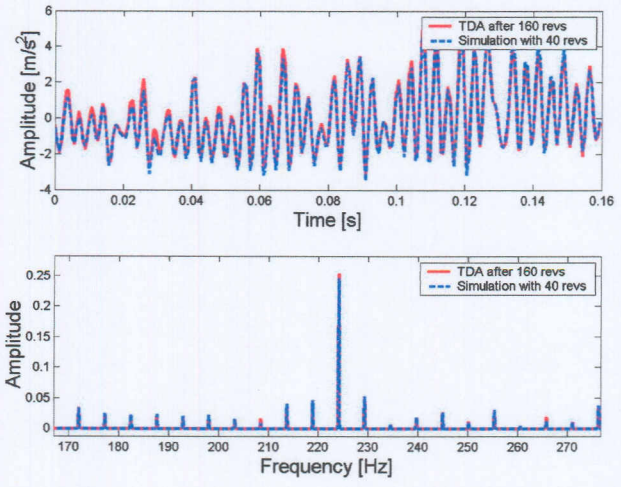

Figure 5.17 (b) Model 1 prediction with validation set of 40 gear rotations superimposed on the TDA from 160 rotations from measurements taken from the constant wear stage of the gear.

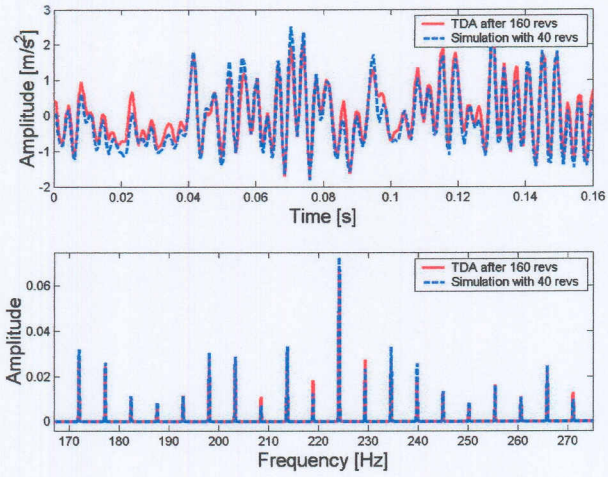

Figure 5.17 (c) Model 1 prediction with validation set of 40 gear rotations superimposed on the TDA from 160 rotations from measurements taken in the wear out stage of the gear.

From above plots it is observed that Model 1 with RBF and 40 gear rotations can predict the TDA for 160 gear rotations fairly well but the prediction of the running in stage of the gear life is poor. This is because the vibration signature of the gear vibration are different and the generalisation capabilities of the selected RBF architecture was not as good as that of MLP network.

Figure 18 (a) to Figure 18 (c) show the results obtained when Model 1 with SVM is simulated using 40 unseen gear rotations for the three different gear life stages.

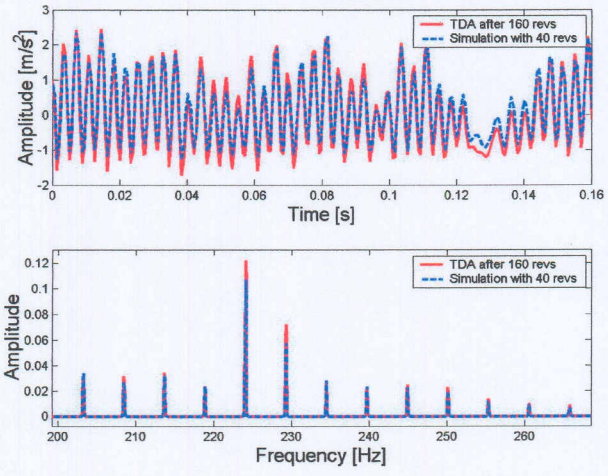

Figure 5.18 (a) Model 1 prediction with validation set of 40 gear rotations superimposed on the TDA from 160 rotations from measurements taken during the running in stage of the gear.

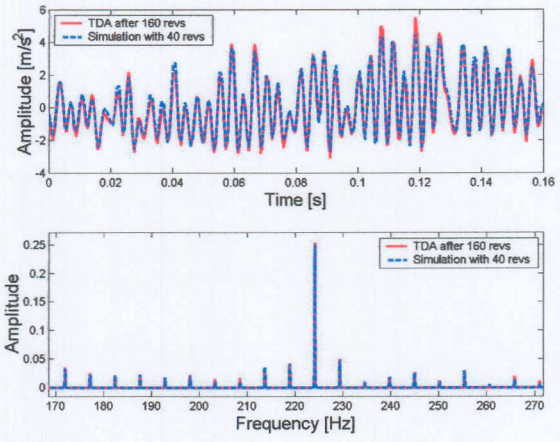

Figure 5.18 (b) Model 1 prediction with validation set of 40 gear rotations superimposed on the TDA from 160 rotations from measurements taken from the constant wear stage of the gear.

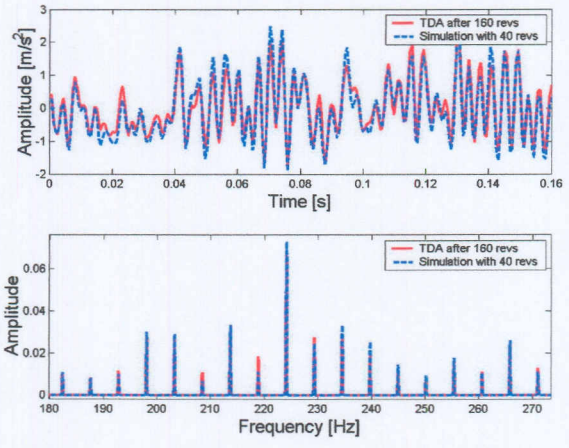

Figure 5.18 (c) Model 1 prediction with validation set of 40 gear rotations superimposed on the TDA from 160 rotations from measurements taken in the wear out stage of the gear.

Model 1 with SVMs produces poor results for the running in stage of the gear life. This is because the vibration signatures of the gear vibration are different in the different stages and the SVM does not generalise well enough.

5.6.2 Simulations with Model 2

In this paragraph Model 2 simulations with unseen validation data from different stages of the gear life are presented.

Figure 19 (a) to Figure 19 (c) show the results obtained when Model 2 with a MLP network is simulated with unseen gear rotations for the three gear life stages.

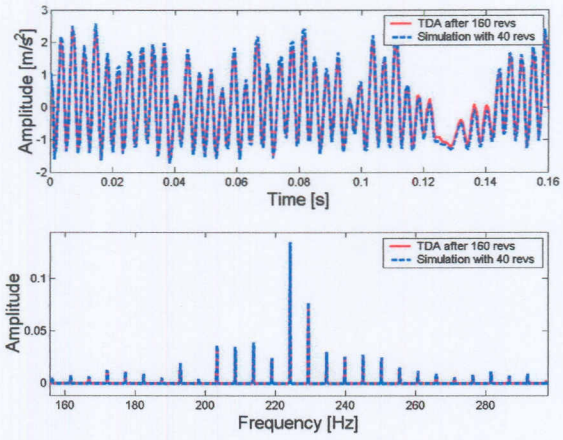

Figure 5.19 (a) Model 2 prediction with a validation set measured during the running in stage of the gear life superimposed on the TDA obtained after 160 gear rotations

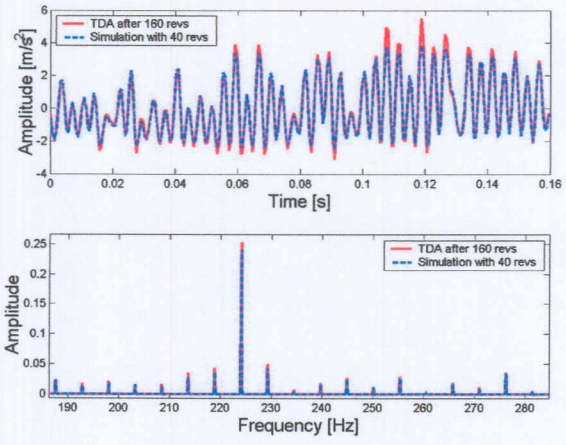

Figure 5.19 (b) Model 2 prediction with a validation set measured during the constant wear stage of the gear life superimposed on the TDA obtained after 160 gear rotations

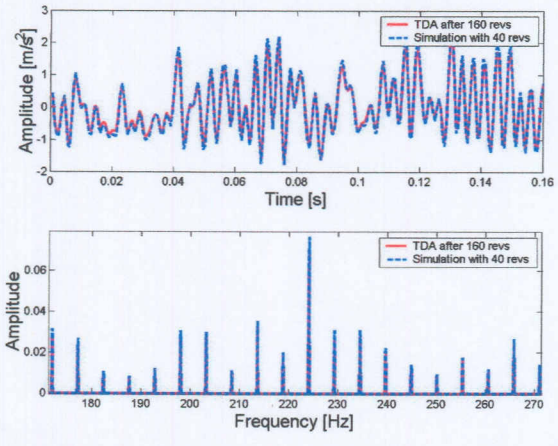

Figure 5.19 (c) Model 2 prediction with a validation set measured during the wear out stage of the gear life superimposed on the TDA obtained after 160 gear rotations

Figure 5.19 (a) to Figure 5.19 (c) show that Model 2 with a MLP feedforward network can correctly predict the TDA for 160 gear rotations over the entire life of the gear. This is because Model 2 uses the whole data set as opposed to Model 1 that uses only a section of the data set.

Figure 20 (a) to Figure 20 (c) show the results obtained when Model 2 with a RBF network is simulated with unseen gear rotations for the three gear life stages.

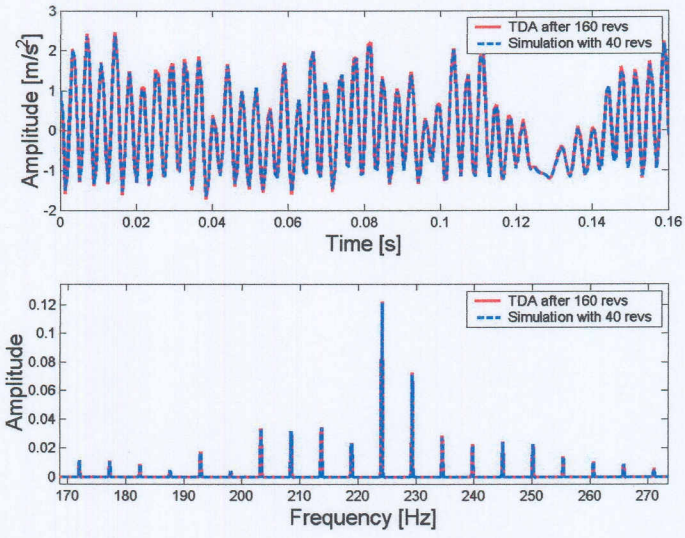

Figure 5.20 (a) Model 2 prediction with a validation set measured during the running in stage of the gear life superimposed on the TDA obtained after 160 gear rotations

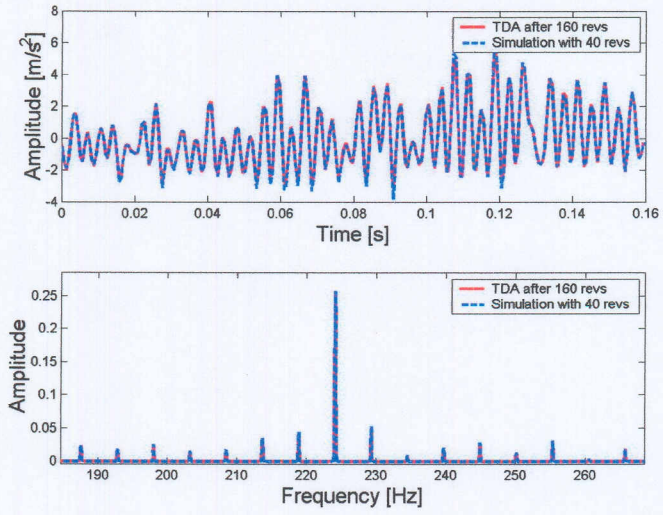

Figure 5.20 (b) Model 2 prediction with a validation set measured during the constant wear stage of the gear life superimposed on the TDA obtained after 160 gear rotations

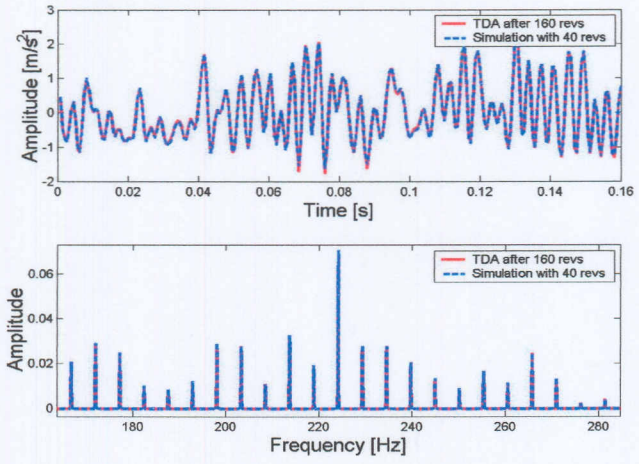

Figure 5.20 (c) Model 2 prediction with a validation set measured during the wear out stage of the gear life superimposed on the TDA obtained after 160 gear rotations

Figure 5.20 (a) to Figure 5.20 (c) show that Model 2 with a RBF feedforward network can correctly predict the TDA for 160 gear rotations over the entire life of the gear. The good performance can again be attributed to the fact that Model 2 uses the whole data during simulation as opposed to Model 1 that uses only a section of the data set.

Figure 21 (a) to Figure 21 (c) show the results obtained when Model 2 with SVMs is simulated with unseen gear rotations for the three gear life stages.

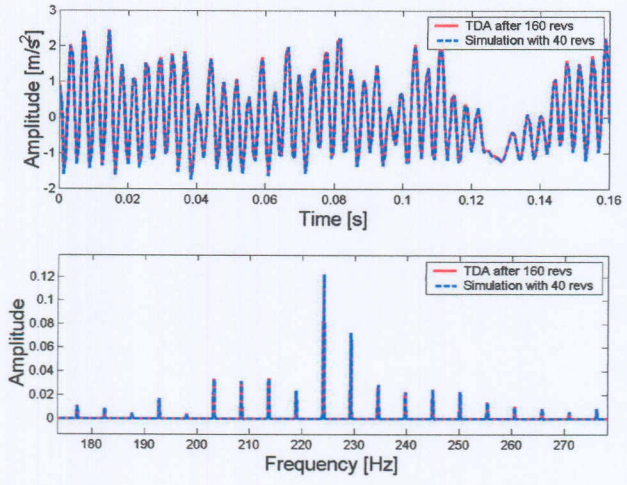

Figure 5.21 (a) Model 2 prediction with a validation set measured during the running in stage of the gear life superimposed on the TDA obtained after 160 gear rotations

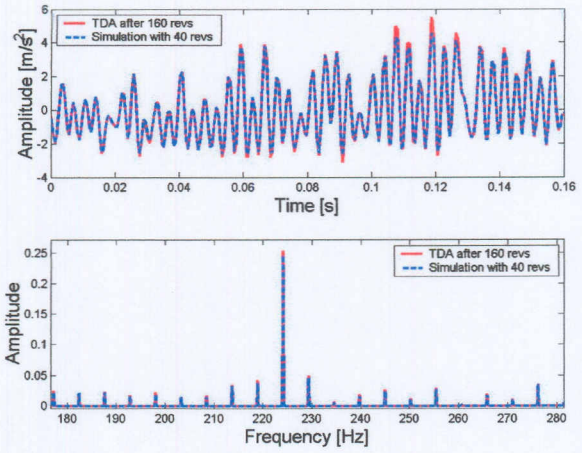

Figure 5.21 (b) Model 2 prediction with a validation set measured during the constant wear stage of the gear life superimposed on the TDA obtained after 160 gear rotations

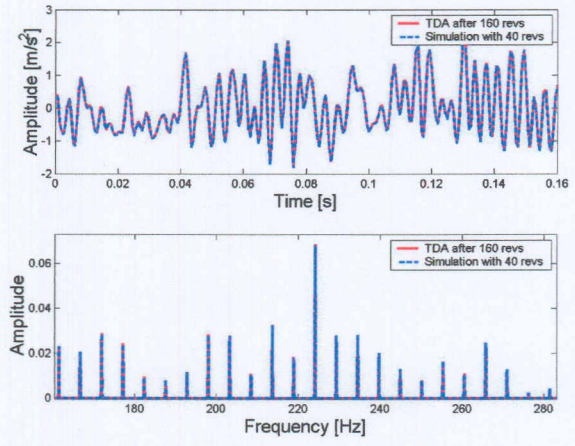

Figure 5.21 (c) Model 2 prediction with a validation set measured during the wear out stage of the gear life superimposed on the TDA obtained after 160 gear rotations

Figure 5.21 (a) to Figure 5.21 (c) show that Model 2 with a SVM network correctly predicts the TDA for 160 gear rotations over the entire life of the gear. The good performance is attributed to the fact that Model 2 uses the whole data during simulation as opposed to Model 1 that uses only a section of the data set.

It is observed from the above plots that ANNs and SVMs can correctly predict the TDA under varying load conditions. This is because when properly trained, ANNs and SVMs can map nonlinearity between an input and output space with good generalisation. Secondly, the applied load was random, therefore, the load modulation on the vibration signature was not synchronous with the vibration of the shaft. This load modulation

condition is called non-synchronous load modulation (Stander and Heyns, 2003) and the TDA can suppress load modulation under non-synchronous fluctuating load conditions because of its randomness relative to the rotation of the gear.

5.6.3 Comparison of the performance of the different formulations under varying load

The performance of the three formulations in Model 1 and Model 2 was assessed using the fit parameter to determine which of the formulations is best suited for this application. Figure 5.22 and Figure 5.23 shows the simulation accuracy η_{sim} plotted against the gear life for Model 1 and Model 2, respectively.

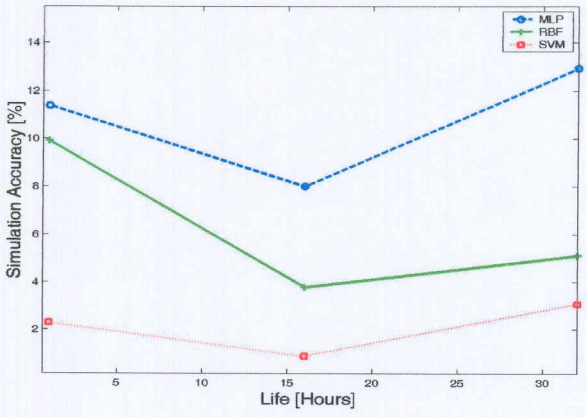

Figure 5. 22 Model 1 Simulation Accuracy η_{sim} vs. gear life

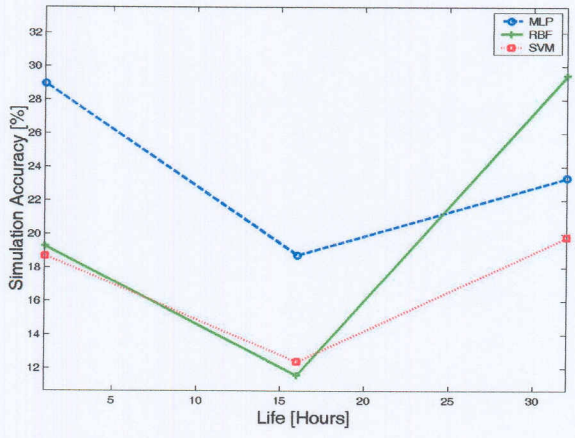

Figure 5. 23 Model 2 Simulation Accuracy η_{sim} vs. gear life

For Model 1 it is observed that SVMs perform best for varying load conditions and MLP gives the worst performance. This is because of the structural risk minimisation used in SVMs, which is said to generalise better than the empirical risk minimisation

used in neural networks (Vapnik 1995; Gunn, 1998). For Model 2 the performance of the formulation is the same. This is because Model 2 uses the whole vibration during simulation therefore the network is exposed to all the transient effects within the data.

The following set of plots compare the performance Model 1 and Model 2 for the different formulations.

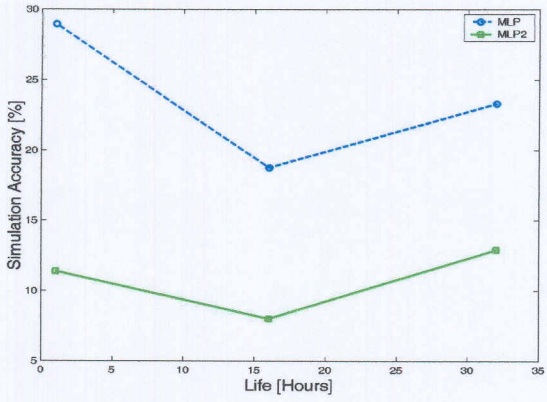

Figure 5.24 Performance of Model 1 and Model 2 with MLP feedforward networks

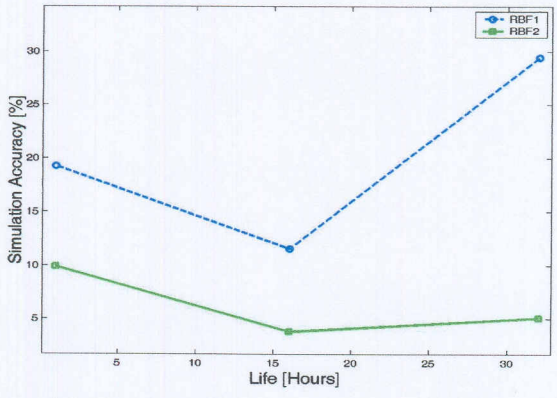

Figure 5.25 Performance of Model 1 and Model 2 with RBF feedforward networks

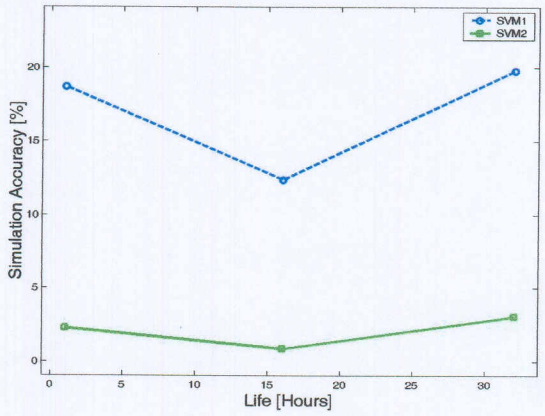

Figure 5.26 Performance of Model 1 and Model 2 with SVM

The above plots show that for varying load condition Model 2 performs much better than Model 1 for all three formulations. This is due to the fact that although Model 2 only uses 10 inputs at a time, it still uses the whole data for simulation as opposed to Model 1 that uses only a section of the data set for simulation. This allows Model 2 to train and simulate more efficiently since it is exposed to all the underlying dynamics within the data set.

5.6.4 Comparison of the diagnostic properties of the TDA calculated by direct averaging and the TDA predicted by the developed models

This paragraph presents the X_{max} and kurtosis to establish whether the TDA predicted by the developed models retains the diagnostic capabilities of the TDA calculated by direct averaging the peak value X_{max} and the kurtosis are used. Figure 5.27 and Figure 5.28 are plots of X_{max} and kurtosis calculated from the TDA predicted by the developed models superimposed on the X_{max} and kurtosis calculated from the TDA calculated using direct averaging for data measured under varying load conditions.

Figure 5.27 shows the results obtained using Model 1 for MLP, RBF and SVMs. In Figure 5.27 and Figure 5.28 X_{max} and kurtosis are only plotted for the running in, constant wear and wear out stages of the gear life. It is observed that the kurtosis is not a good fit. This implies that Model 1 cannot be used to monitor the presence of impulses in the gear vibration. The peak values for TDA calculated using direct averaging and the peak values for TDA obtained using Model 1 fit well. This implies that the peak values of the TDA obtained using Model 1 can be used to monitor the overall vibration of the gear signal.

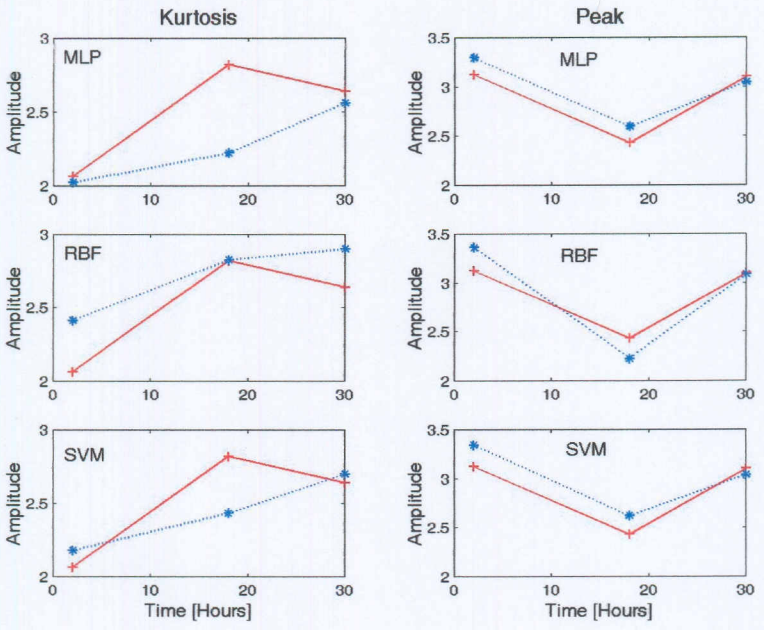

Figure 5.27 Comparison of kurtosis and peak values for the TDA calculated by direct averaging (solid line) and the TDA predicted by Model 1 (dotted line) with MLP, RBF and SVMs.

Figure 5.28 shows the results obtained using Model 2 for MLP, RBF and SVMs during the running in, constant wear and wear out stages of gear life.

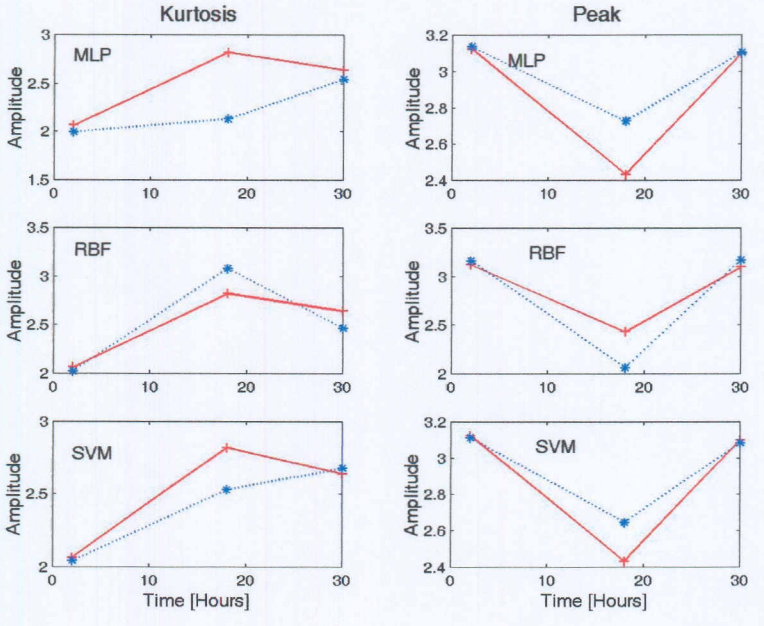

Figure 5.28 Comparison of kurtosis and peak values for the TDA calculated by direct averaging (solid line) and the TDA predicted by Model 1 (dotted line) with MLP, RBF and SVMs.

It is observed from Figure 5.28 that both the kurtosis and the peak values are not far off. This implies that the TDA predicted by Model 2 can be used to monitor impulses and the overall gear vibration. The superior performance of Model 2 is attributed to the fact that Model 2 exposes the formulations to the entire vibration during the simulation process. Table 5.2 and Table 5.3 present a summary of the properties of Model 1 and Model 2 for the three formulations.

Table 5.2 Summary of properties for Model 1 with MLP, RBF and SVMs.

	Strength	Weaknesses	Ideal application
MLP	Good generalisation under constant load conditions Good generalisation under varying load conditions	Depends on training and generalisation of selected network	Monitoring of overall vibration and impulses in a gear vibration under constant load conditions Monitoring of peak values under varying load conditions
RBF	Good generalisation under constant load conditions	Poor generalisation under varying load conditions Depends on generalisation of selected network	Monitoring of overall vibration and impulses constant loading conditions Monitoring of peak values under varying load conditions
SVM	Good generalisation under constant load conditions Good generalisation under varying load conditions	Depends on generalisation of SVM	Monitoring of overall vibration and impulses under constant loading conditions Monitoring of peak values under varying load conditions

Table 5.3 Summary of properties for Model 2 with MLP, RBF and SVMs

	Strength	Weaknesses	Ideal application
MLP	Good generalisation under constant load conditions Good generalisation under varying load conditions	Looses diagnostic capability for overall vibration under varying loads Depends on generalisation of selected network	Monitoring of overall vibration and impulses in under both constant and varying load conditions
RBF	Good generalisation under constant load conditions Good generalisation under varying load conditions	Poor generalisation under varying load conditions Looses diagnostic capability for overall vibration under varying loads Depends on generalisation of selected network	Monitoring of overall vibration and impulses in under both constant and varying load conditions
SVM	Good generalisation under constant load conditions Good generalisation under varying load conditions	Depends on generalisation of SVM	Monitoring of overall vibration and impulses in under both constant and varying load conditions

5.7 Conclusion

In this chapter the synchronous filter for time domain averaging of gear vibration data developed in Chapter 4 is tested on a new vibration data set from the accelerated gear life test rig to assess its suitability for use over the entire life of the gear. For measurements from tests carried out under constant load conditions the performances of Model 1 and Model 2 are practically the same over the entire life of the gear. For measurements from a test carried out under varying load conditions Model 2 performs better than Model 1 over the entire life of the gear. The superior performance of Model 2 is because Model 2 uses the whole data set for training and simulation as opposed to Model 1, which uses only a section of the data set. Using the whole data set during training and simulation exposes the formulations in the model to all transient effects within the data resulting in a more accurate TDA prediction. The performance of Model 1 strongly depends on the generalisation capabilities of the formulation that is used.